energies

MDPI

Article

Design of an Anti-Corona Device for HVAC Substation Connectors

Ane Miren Larrea, Manuel De La Hoz, Agurtzane Etxegarai, Angel Javier Mazon * and Itxaso Aranzabal

Department of Electrical Engineering, Faculty of Engineering of Bilbao, University of the Basque Country UPV/EHU, 48013 Bilbao, Spain
* Correspondence: javier.mazon@ehu.eus

Abstract: One of the aspects to consider during high-voltage (HV) equipment design is the reduction in the probability of corona effect onset. Indeed, the corona effect is related to high electric field values beyond the equipment's insulation levels and insulation strength, among other factors. This issue can be addressed during the design step, either by modifying the geometry of the electrical device or by including additional elements in the equipment structure to smooth out the voltage gradient along critical regions, such as anti-corona devices. The study of anti-corona devices for HV insulators is well documented, in contrast to substation connectors. Therefore, the present study proposed the design of a novel anti-corona device for HV substation connectors, including a method for the selection of its dimensions. This study shows that the relationship between the dimensional design variables and the critical electrical field on the connector is described by linear and rational functions. Thus, the design process times are cut down due to a reduction in the number of simulations required to run the assessment of the anti-corona device arrangement impact.

Keywords: computer-aided manufacturing; connector; corona ring; electric fields; high voltage

Citation: Larrea, A.M.; De La Hoz, M.; Etxegarai, A.; Mazon, A.J.; Aranzabal, I. Design of an Anti-Corona Device for HVAC Substation Connectors. *Energies* **2022**, *15*, 5781. https://doi.org/10.3390/en15165781

Academic Editors: Meng Huang, Yunxiao Zhang and Chenyuan Teng

Received: 18 July 2022
Accepted: 4 August 2022
Published: 9 August 2022

1. Introduction

The appearance of the corona effect is common in high-voltage (HV) overhead lines. The phenomenon corresponds to a discharge at the point where the electric field is greater than the disruptive strength of the insulation that surrounds the surface of the conductor and has several physical aspects, such as sound, luminance, and electromagnetic pulse waves that produce energy losses on the transmission system [1]. In the worst case, a corona effect could develop into an arc that causes the destruction of electric devices installed in overhead lines, such as insulators or connectors [2,3].

The study of the corona effect involves the calculation of the maximum electric field that insulation can withstand, which is a common step in the design of HV installations (e.g., substations) [4] and HV equipment (e.g., switchgear, insulators, connectors) [5]. The tools used in power system analysis studies generally include approximated modelling regarding the geometries of the transmission lines and towers [6]. However, in some specific geometries of insulators and connectors, a more detailed analysis is required [7,8]. In all cases, finite element analysis (FEA) is a valuable tool for calculating the electric field distribution.

The electric field that is generated at the surface and around insulators and line connectors depends directly on the applied voltage and the geometry of the electrode. However, it is necessary to consider the environmental and insulation conditions to understand the corona effect completely [7]. Connectors are only subject to the line voltage, whereas in the case of insulators, one end is connected to the line voltage and the other end is grounded. The large difference in the voltage supported by the insulators causes an electric field gradient [9]. In contrast, for connectors, it is due to the smaller curvature in their geometry [10] since there is no voltage difference over them.

The installation of anti-corona devices for insulators is well documented in the literature. In the case of insulating strings, Ilhan and Ozdemir [11] considered the electric

field surface of different points from the grading ring and the insulator string. Then, based on a sensitivity analysis, possible solutions were tested by considering the radio interference voltage produced by the configuration. Other authors applied optimisation methods [12]. However, these works did not show an evident solution to the location and size of the corona rings. Proposed optimisation algorithms are the bat flying algorithm [13], particle swarm optimisation [14,15], and surface response [16]. Generally, some minimum electrical field value is considered as an objective at a particularly critical point (e.g., the insulation triple point of an insulating string [17]) or along a characteristic line length (e.g., the periphery line of the insulating string [18]). Regarding the corona effect onset at substation connectors, Guiteras et al. [19] suggested installing shielding parts around the connectors or to cover them with a spherical cage under the same voltage. This solution reduces the electric field, and therefore, it can be used on systems operating under higher voltage. Nevertheless, for the specific problem conditions, the authors concluded that a redesign of the geometry of the connector is preferred. This approach is only valid for certain connectors since it may not be feasible for certain conductor arrangements. The redesign of the connectors also implies another kind of study for the connector (thermal, mechanical, etc.), and therefore, more industrial tests to be carried out.

Three essential requirements are desirable in the design, manufacturing, and installation of corona rings. First, the rings must be simple to build. Second, the installation of the corona rings on site must be straightforward, involving a minimal number of steps. Consequently, in the present study, unconventional surfaces were not analysed, such as in Pattanadech et al. [20] and Liao et al. [21]. However, it could be a valid type of optimisation when applied to insulators [22]. Third, the point of attachment of the toroid is also relevant. Its position in space must be supported by some object to which it can be mechanically linked using an adjustment to achieve fixation [23]. For connectors, this means using their civil work support, if they have one, or fixing the rings on the conductors that enter the connector. The last option was considered for this work.

Other time minimisation techniques in the test development are implemented in the modelling of anti-corona rings, such as the design of experiments (DOE) and analysis of variance (ANOVA) [16], in this case, for insulators. The limitation of this method lies in the fact that the relationships between the multiple factors considered must be linear [24].

The present study proposed the design of a novel anti-corona device, i.e., an anti-corona ring, for HV substation connectors, including a method for ring dimension selection. The corona ring shape was mainly selected because it is easier to manufacture and maintain compared with spherical cages or other geometries.

The applied method was focused on considering whether algorithmic expressions can be derived for the sizing of corona rings to reduce the analysis time in the design stage, as well as applying it to usual cases on substation connectors. It reduces the design process calculations by considering the relationship between the geometric dimensions of the corona rings and the value of the maximum surface electric field of the substation connector near the anti-corona ring. The objective was to reduce the number of trials to establish the possible relationship between design parameters, thus minimising the simulation resources required for an iterative optimisation process.

The other advantage comes from the simulation of testing conditions using FEA. Although we considered the electrical field only at the connector surface, the connector geometry is challenging to model and must be done without any dimensional simplification (from a three-dimensional model to an axis-symmetry one, for instance). Any reduction in the numerical methods required speeds up the design process and increases the possibility of reduced testing.

This paper is organised as follows. In the first part, geometrical details of the substation connectors, testing setup, and the anti-corona device arrangement are introduced. Thus, a numerical FEA model that was used to simulate standard HV laboratory conditions is presented, and the location of the maximum surface electric field is given. Based on previous results, in the second part, the specific positions of the corona rings near the

substation connectors under study that reduced the electric field are given. The results of several simulations to determine the effect of the proposed anti-corona ring's geometrical factors on the electric field are presented. The last part offers information about the algebraic relationship between variables that diminish the design time, reduce the number of simulations, and consider the surface electric field as an indicator. The method can also be used on site to improve the location of the corona rings for standard conditions.

2. Description of the Connectors and the Testing Setup

2.1. Geometry of the Connectors and the Testing Setup

The novel anti-corona device proposed in the present study was investigated for its application in specific aluminium connectors used in HV electrical substations. However, the arrangement is valid for any substation connector provided that a corona ring is installed in each of the connectors coupled through a substation connector following the design method introduced in Section 4.

The connectors under study are shown in Figure 1, where their main dimensions are defined, including their length, width, height, and minimum radius. The dimensions of each connector are shown in Table 1.

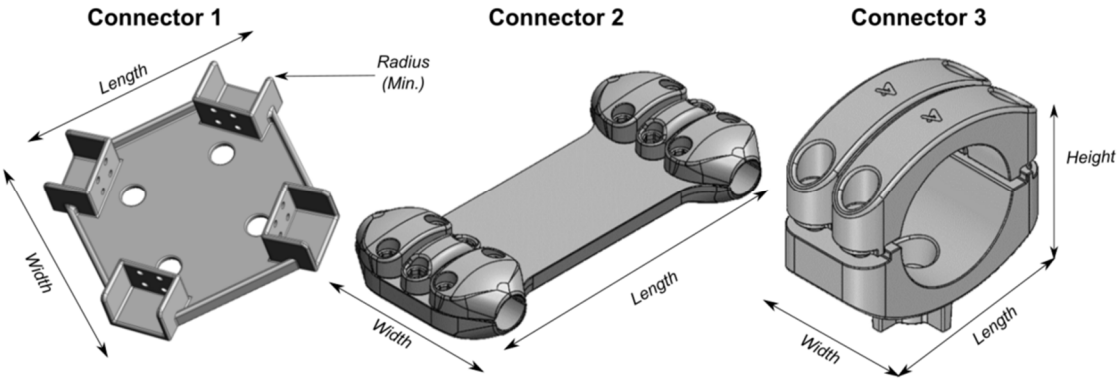

Figure 1. Geometry of connectors.

Table 1. Geometrical dimensions of connectors.

Connector	Length (mm)	Width (mm)	Height (mm)	Radius Min. (mm)
Connector 1	470	470	100	6
Connector 2	585	270	95	3
Connector 3	240	120	230	4

In the present study, the investigation of the electric field around the connectors was based on the recreation of a laboratory testing setup, as shown in Figure 2. In the testing arrangement, several tubes allowed the connector to be suspended in the model, reflecting its possible installation in the substation, which would be the conventional assembly to be tested in the laboratory. Their diameters are the same as those used under standard installation requirements.

One of the simplest and most effective solutions to reducing the electrical stress generated at the ends of the conductors in the test bench is to use corona-shielding systems (spheres and rings) at their ends [25] to prevent the electric field from increasing dramatically. Generally, these metal parts have a ring, spherical, or bowl shape [8]. Note that these elements are independent of the corona rings. The testing enclosure consisted of a box with dimensions 15 m $\times$ 15 m $\times$ 10 m and the arrangement was located at the centre, as shown in Figure 2.

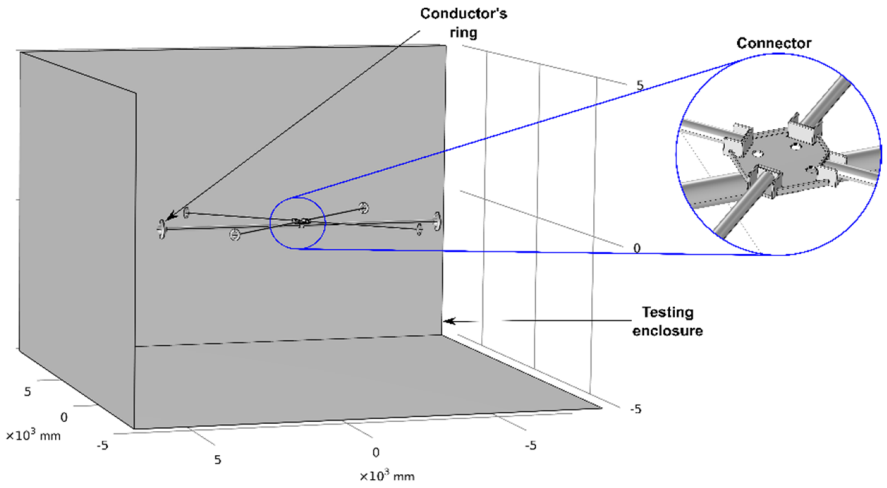

Figure 2. Modelled setup for the connectors. The box represents the testing room.

2.2. Configuration of the Simulation Tool

The electric field of the connector was calculated with FEA. The assumptions considered were as follows. First, the FEA model simulation was carried out under HV laboratory conditions, according to normal pressure, temperature, and humidity, as established in standard IEC 61284 [26]. The FEA software tool of preference for this work was COMSOL Multiphysics.

Second, when simulating a piece that is connected to conductors, its ends are exposed. That is, an infinite conductor cannot be defined. However, this had no impact when evaluating the piece, provided its length is considerably longer than the connector under analysis. Even so, a sphere covered the ends to avoid the maximum electric field of the whole assembly being found at the ends of the conductor, given its sharp geometry.

The testing setup in Figure 2 was modelled in the FEA software. Then, the electric field was only analysed at its most critical point, i.e., the maximum values at each point of the connector surface were identified, omitting the fact that the voltage varied over time (the maximum value is at the peak of the sinusoidal wave).

The simulation enclosure was grounded to define an appropriate environment. The rest of the pieces were connected to a line voltage of 450 kV_{peak} as the reference.

The characteristics of the mesh are a key factor when carrying out an analysis by means of FEA. To obtain precise results, the "very fine mesh" option in the meshing stage on COMSOL Multiphysics was selected. Other important characteristics related to the type of mesh used are described in Annex I.

After defining meshing characteristics, a stationary study was carried out. Once the electric field on the connector was calculated, the point with the highest electric field value was obtained.

3. Geometry and Design of the Anti-Corona Device

3.1. Geometry of the Anti-Corona Device

The electric field depends directly on the geometry of a power system element under voltage. Therefore, if the geometry of the element is varied, it has an impact on its electric field. To reduce the electric field of substation connectors, the present study proposed to include a ring around each conductor (Figure 3). In this way, it was possible to alter the geometry of the whole assembly (connector, rings, and conductors) and, in turn, the electric field. By attaching the rings to the conductors, a stable hold was allowed. Thus, a distance was kept between the ring and the connector, as defined by the designer. The ring arrangement presented in this work allowed for a straightforward replacement of the rings if necessary and a perfect fastening at a distance from the piece as determined by the designer. In this way, the same connector could be used under different operation conditions by changing the geometry or distance of the rings instead of changing or

redesigning the connector. In addition, compared with spherical cages, rings are easier to manufacture and maintain.

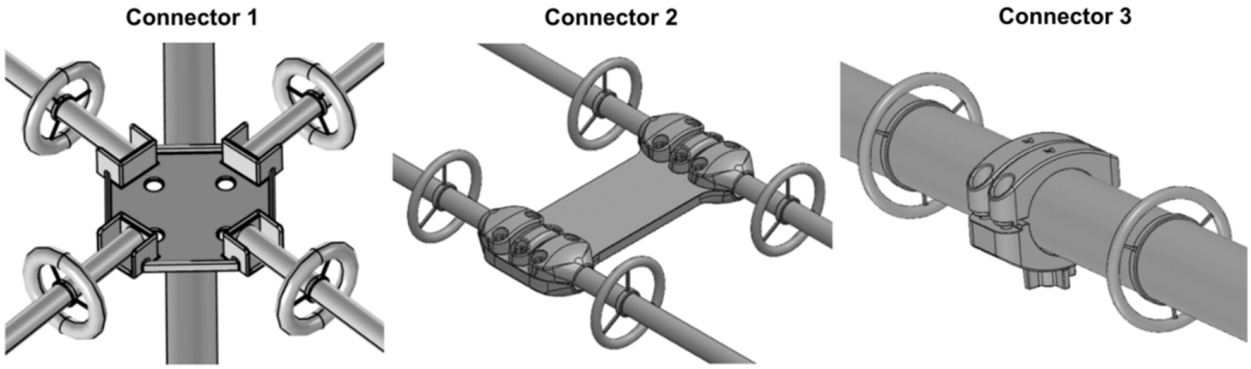

Figure 3. Connector with rings installed around the conductors.

The design of the anti-corona device was classified according to the following parameters: thickness of the rings (A), inner diameter of the rings (Dint), and distance between the ring and the connector (dist), as identified in Figure 4.

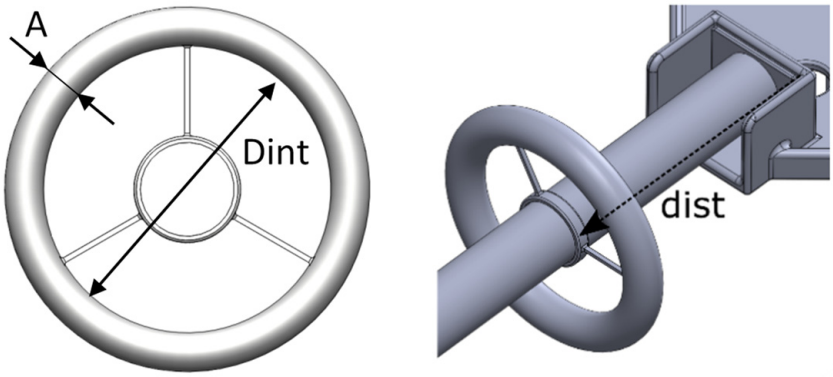

Figure 4. Design of individual rings installed around the conductors.

3.2. Modelling and Simulation of the Setup with the Anti-Corona Device

The electric field of the connector was calculated with FEA again, but now for several cases that considered different parameter values. First, the testing setup in Figure 2 with the anti-corona device was modelled in the FEA software again. Then, the maximum electric field in the position found in Section 2.2 has been recorded. Two of the parameters were always constant and the last one was modified in order to find out the dependency with the maximum electric field on the connector surface.

The simulation enclosure was grounded to define an appropriate environment. The rest of the pieces were connected to a line voltage of 450 kV_{peak} as a reference, including the anti-corona device, since it was fixed to the cables of the setup.

4. Simulation Results

4.1. Simulation Results without the Anti-Corona Device

The electric field at the surface of the connectors under study without any anti-corona device installed is shown in Figure 5. It can be observed that the maximum electric field value mostly occurred in the zone with the highest curvature. However, the normal vector from these critical surfaces was not always in the same direction as the axis of the tubes, as shown for connector 3 in Figure 5.

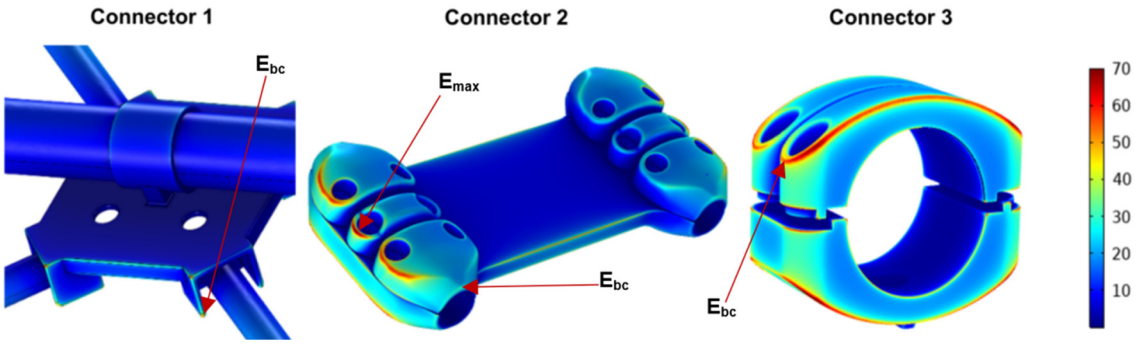

Figure 5. Electric field (kV/cm) at the connector surface.

The maximum field values at the surface of the connectors without any ring were 45.2 kV/cm (connector 1), 46.5 kV/cm (connector 2), and 65.3 kV/cm (connector 3).

The point of evaluation of the electric field for the simulations in Section 4.2 is indicated in Figure 5 by E_{bc}. It coincided with the location of the maximum electric field E_{max}, except in the study of connector 2. The proposed solution reduced the electric field magnitude in the closest points to the rings and the electric field vector must be almost parallel to the ring axis. Therefore, for connector 2, the point selected to analyse E_{bc} was a point near the plane of the anti-corona device installation with an electric field value of 20.0 kV/cm.

4.2. Simulation Results with an Anti-Corona Device

For the different configurations in Figure 3, several simulations were carried out by changing the ring parameters: thickness (A), inner diameter (Dint), and distance between the ring and the connector (dist). Figure 6 describes the maximum electric field value found at the connector surface under each specific parameter while keeping the others constant. It can be noted that for any configuration with anti-corona devices, the electric field was weaker than without the anti-corona devices, as indicated in Section 4.1, and the corona inception voltage was also reduced.

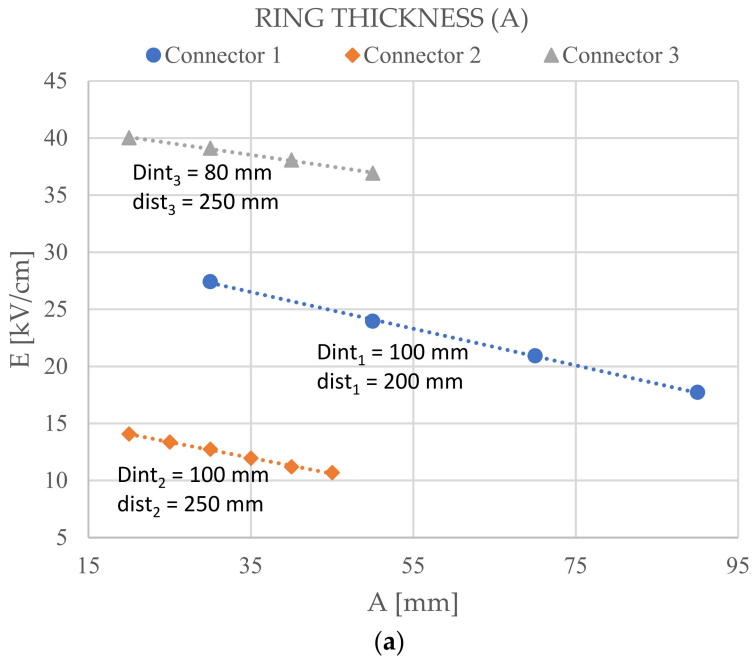

(**a**)

Figure 6. *Cont.*

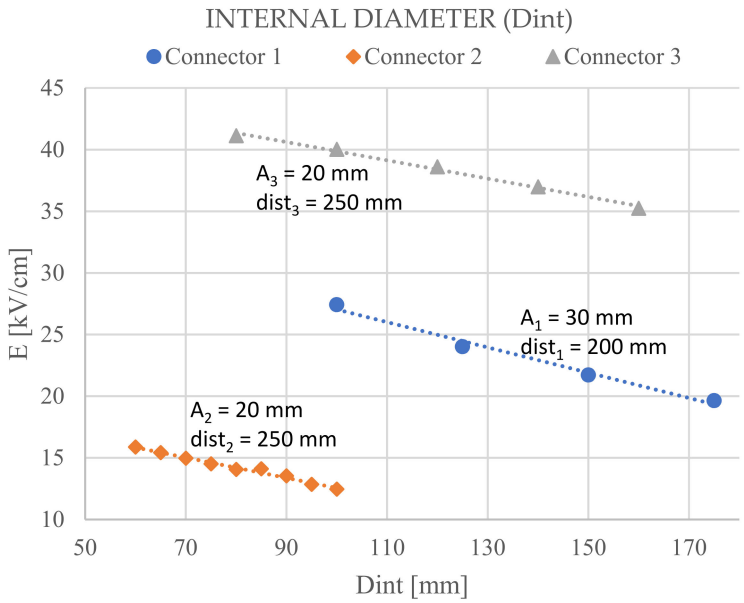

(**b**)

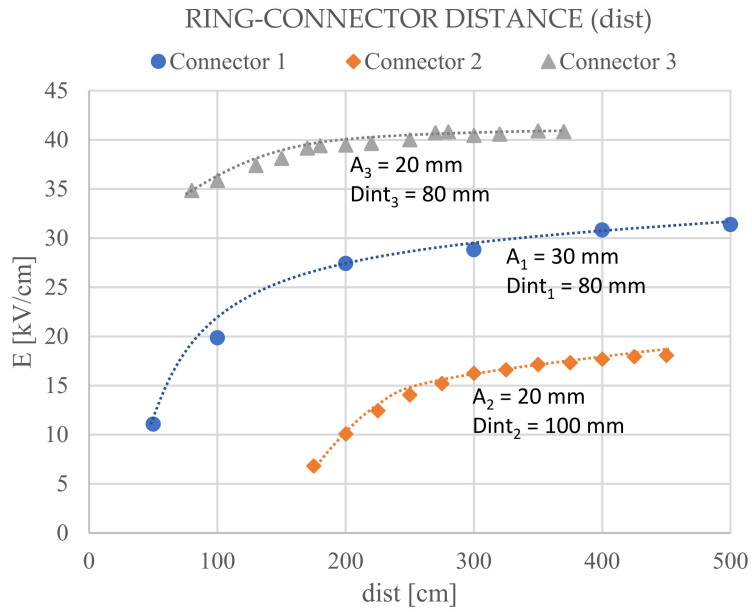

(**c**)

Figure 6. Electric field on the connector's surface as a function of the ring dimensions: (**a**) ring thickness, (**b**) internal diameter, and (**c**) ring–connector distance.

Even if the sweep range was modified for the different study cases, the tendency was similar for each parameter study. Depending on the electric field present at the installation point of the anti-corona device, the results of Figure 6 allowed for deciding the dimensional characteristics of the anti-corona device as a first approximation.

As observed in Figure 6a, the change in thickness of the ring (keeping its internal diameter constant) followed a downward linear trend. Analogously to the thickness, the increase in the internal diameter of the ring (Figure 6b) followed the same trend. Thus, the larger the internal diameter of the rings (keeping the rest of the parameters constant), the smaller the electric field. Finally, the variation of the distance between the ring and the connector in Figure 6c did not follow a linear trend, but a more complex trend. It was verified that the farther the rings were from the connector, the less influence they had on the electric field.

For a more accurate design, three fitting equations were extrapolated from Figure 6 based on the parameters analysed and the maximum electric field value. Equations (1)–(3) are intended for the selection of the corona ring dimensions. Equations (1) and (2) correspond to the relationships between the electric field E (kV/cm) and ring thickness A (mm) and between the electric field E (kV/cm) and the internal diameter of the ring Dint (mm). Equation (3) relates the electric field E (kV/cm) and the distance between rings and connectors dist (mm). The value of R^2 for all the fittings was above 0.92. The constant values C1 to C6 according to the connector and equation are shown in Table 2.

$$E_{max} = C1 \times A + C2 \quad (1)$$

$$E_{max} = C3 \times Dint + C4 \quad (2)$$

$$E_{max} = \frac{C5}{\sqrt{dist}} + C6 \quad (3)$$

Table 2. Constant values of Equations (1) to (3) for each connector.

Connector	C1	C2	C3	C4	C5	C6
Connector 1	−0.161	32.1	−0.103	37.3	−212	41.3
Connector 2	−0.138	16.8	−0.082	20.8	−376	36.9
Connector 3	−0.103	42.1	−0.074	47.3	−106	46.78

In Equations (1)–(3), the other parameters are kept constant, as specified in Table 2. A single fitted Equation (4) was deduced for the most general case, where all the parameters are described together. The constant values L1 to L4 for each connector are shown in Table 3.

$$E_{max} = \mathrm{L1} + \mathrm{L2} \times A + \mathrm{L3} \times Dint + \frac{L4}{\sqrt{dist}} \quad (4)$$

Table 3. Constant values of Equation (4) for each connector.

Connector	L1	L2	L3	L4
Connector 1	56.8	−0.161	−0.103	−212
Connector 2	46.8	−0.138	−0.082	−376
Connector 3	56.2	−0.103	−0.074	−106

Equation (4) is useful for determining the electric field in a combination of the parameters that are not included in the studied cases, as long as the case considered is an interpolation.

The distance between the rings and the connector (dist) is a key factor when studying the adequacy of an anti-corona device. If physical restrictions are disregarded, the closer the rings are to the piece, the smaller the electric field. In case the electric field value is not sufficiently low, the rings would have to be replaced by other rings of greater thickness or greater internal diameter.

5. Discussion

Based on the configuration of a specific connector, it is possible to avoid the appearance of the corona effect by decreasing the value of the electric field at its surface. For this purpose, the present study proposed installing corona rings around each conductor linked by the connector. Under these conditions, the inception voltage increased, allowing for use of this equipment in applications with a higher electrical voltage. The geometry of the rings was defined by three parameters: thickness (A), internal diameter (Dint), and distance (dist), which can be calculated separately using Equations (1)–(3) for the connectors investigated in this study (Figure 1). The equations were verified for the connectors under study, which were subjected to a line voltage of 450 kV_{peak} AC. The procedure can be generalised, and

thus, it can be applied to other connector designs at any voltage level. The generalised design methodology is introduced in the present paper.

The paper presents other contributions, too. First, the maximum electric field under some conditions (e.g., connector 2) was not located in a favourable position for the anti-corona ring to reduce its magnitude by a considerable percentage. The electric field reduction was strongly influenced by the separation between the anti-corona ring and the connector point under study. Hence, for very long connectors, the solution introduced in the present work could be impractical. Alternatively, the anti-corona ring can circumscribe the point where the electric field needs to be attenuated. However, the fixation of the ring should be further studied.

Moreover, the design of the corona rings suggests the possibility of optimisation. Equation (4) gives a tentative objective function, where both economic and technical aspects should be considered. In any case, a sweep over each of the study cases is useful to analyse the behaviour of all the variables together, as shown in Figure 7. In each axis of Figure 7, one of the parameters involved in Equation (4) is represented. The electric field of each square has a colour that represents its value and corresponds to the case with the midpoint combination values. The hypersurface does not allow for inferring the behaviour of the design parameters analytically, but it does offer a global idea of the corona ring designs that should be considered by the designer. For instance, we could quickly establish areas with a limit value (e.g., 30 kV/cm) and discard those designs on the hypersurface.

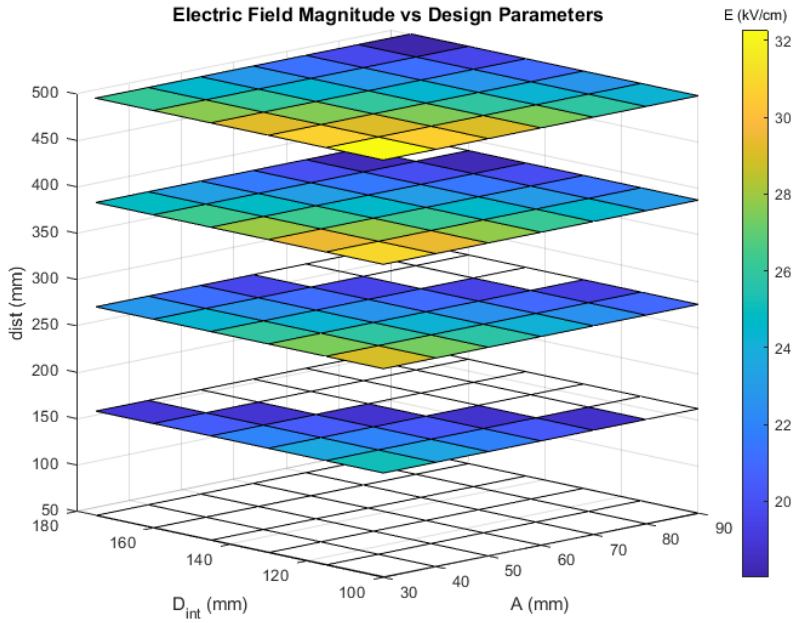

Figure 7. Electric field on connector 1 as a function of the ring dimensions: thickness (A), internal diameter (Dint), and ring–connector distance (dist), represented simultaneously.

6. Conclusions

The installation of corona rings around a device to protect it, e.g., HV substation connectors, is a simple and effective way to avoid the appearance of the corona effect. The rings decrease the electric field at the critical points, and consequently, the probability of the corona effect occurring. The present study proposed a novel anti-corona device arrangement consisting of the installation of a corona ring per conductor coupled through substation connectors. This anti-corona device guaranteed a correct fixation and the corona effect onset was reduced. The design was studied for specific connectors used for the connection of four conductors under a line voltage of 450 kV_{peak} AC.

The design of corona devices is a key factor when evaluating the electric field at a substation connector or in the case of substation repowering. Therefore, several simulations were carried out in the present work in order to determine the most adequate anti-corona

device design for a lower electric field. Three design parameters were considered, which were related to the geometrical configuration: the thickness, internal diameter, and proximity of the rings. It was demonstrated that by increasing the thickness or internal diameter of the rings, the electric field was reduced. The decrease in the electric field could also be achieved by bringing the rings closer to the connector. Hence, all three design parameters were essential when designing the proposed anti-corona device. In addition, it was hereby shown that the relationship between the maximum electric field value of the connector and the internal thickness or diameter of the ring followed a decreasing linear trend. However, the relationship with distance was proportional to the inverse square root.

Based on the simulation results of the present study, it was concluded that the behaviour of the surface electric field was monotonous and had no tendency towards producing valleys or ridges. However, the combination of the aforementioned three design variables is the final decision of the designer, who in turn will have to take other factors into account. Thus, the disposition and dimensions of the anti-corona device must be defined by the designer with the aid of the method presented in this paper. Therefore, fitting equations were introduced to be used for the optimal design of the rings for a given connector as part of a design method. This can avoid needing to run an FEM simulation for each anti-corona device to be installed. Non-linear regression was used assuming control of the variables, then extrapolating said expression in a linear combination, assuming interdependence between the variables involved. This approach improved the prediction precision at the expense of simulation time. In any case, it is more adequate than an iterative optimisation process.

The design of the anti-corona device to reduce the electric field suggests the possibility of optimisation. A general equation was proposed in this study, and it could give a tentative objective function. The economic and technical factors will imply other parameters of importance. However, a sweep over each of the cases with the available information can be useful to observe the behaviour of all the parameters together.

7. Annex I—Mesh Statistics and Hardware Used

Every mesh has different conditions due to the connector shape, size, and details. Nevertheless, we averaged such values to provide detail of the meshing characteristics, as shown in Table 4. All the discrete elements were tetrahedral, and they were second order. The machine used in the simulations had the following specifications: Dell Precision Tower 7810, Intel Xeon E5-2620 v4 processor, 16 GB DDR4 RAM at 2400 MHz, two SSDs (Dell Europe, manufacturing country Spain, manufacturing date 01/12/2018), one hard disc Samsung PM87 of 500 GB SATA, one hard disc Samsung 250 GB NVMe 970 EVO Plus, and an Nvidia Quadro K1200 video card. The average simulation time was around 40 min for each case under these circumstances.

Table 4. Average mesh statistics of FEM models used.

Feature	Value
Maximum element size	300 mm
Minimum element size	3 mm
Maximum element growth rate	1.3
Curvature factor	0.2
Resolution of narrow regions	1 mm
Mesh vertices	2,193,218
Number of domain elements	12,206,278
Number of boundary elements	1,176,207
Number of edge elements	31,275
Number of points elements	1006
Skewness	0.656
Maximum angle	0.736
Volume vs. circumradius	0.669
Volume vs. length	0.765
Condition number	0.826
Grow rate	0.551

Author Contributions: Conceptualisation, A.M.L., M.D.L.H. and A.E.; methodology, M.D.L.H., A.J.M. and A.E.; software, A.M.L. and M.D.L.H.; formal analysis, A.J.M. and I.A.; writing—original draft preparation, A.E.; writing—review and editing, A.E. and I.A.; funding acquisition, A.J.M. All authors have read and agreed to the published version of the manuscript.

Funding: The authors wish to thank the support from the Basque Government (GISEL research group IT1191-19 and ELEKTRIKER research group IT164-22), as well as from the University of the Basque Country UPV/EHU (GISEL research group GIU18/181 and ELEKTRIKER research group GIU20/034).

Conflicts of Interest: The authors declare no conflict of interest.

References

1. Giao, T.N.; Jordan, J.B. Modes of Corona Discharges in Air. *IEEE Trans. Power Appar. Syst.* **1968**, *Volume PAS-87*, 1207–1215. [CrossRef]
2. Goldman, M.; Sigmond, R.S. Corona and Insulation. In *IEEE Transactions on Electrical Insulation 1982*; IEEE: Toulouse, France, 1982; Volume EI-17, pp. 90–105. [CrossRef]
3. Rao, R.D.; Chinda, P.R.; Kiran, M. Corona and Electric Field Distribution Analysis in 400 kV Line Insulators. *Adv. Technol. Innov.* **2020**, *6*, 21. [CrossRef]
4. Zhang, S.; Fan, Y.; Lei, Q.; Wang, J.; Liu, Y.; Zhan, T. Insulation structure design and electric field simulation of 500 kV isolation energy supply transformer for HVDC breaker. *High Volt.* **2022**, *7*, 185–196. [CrossRef]
5. Nayak, M.R.; Radhika, G.; Devulal, B.; Reddy, P.D.; Suresh, G. Optimization of high voltage electrodes for 765 kV bus post insulators. *Sustain. Energy Technol. Assess.* **2021**, *47*, 101529. [CrossRef]
6. Li, Q.; Rowland, S.M.; Shuttleworth, R. Calculating the Surface Potential Gradient of Overhead Line Conductors. *IEEE Trans. Power Deliv.* **2015**, *30*, 43–52. [CrossRef]
7. Olsen, R.G.; Tuominen, M.W.; Leman, J.T. On Corona Testing of High-Voltage Hardware Using Laboratory Testing and/or Simulation. *IEEE Trans. Power Deliv.* **2018**, *33*, 1707–1715. [CrossRef]
8. Wang, J.; Yue, B.; Deng, X.; Liu, T.; Peng, Z. Electric field evaluation and optimization of shielding electrodes for high voltage apparatus in ±1100 kV indoor DC yard. *IEEE Trans. Dielectr. Electr. Insul.* **2018**, *25*, 321–329. [CrossRef]
9. Phillips, A.J.; Maxwell, A.J.; Engelbrecht, C.S.; Gutman, I. Electric-Field Limits for the Design of Grading Rings for Composite Line Insulators. *IEEE Trans. Power Deliv.* **2015**, *30*, 1110–1118. [CrossRef]
10. Hernandez-Guiteras, J.; Riba, J.; Casals-Torrens, P. Determination of the corona inception voltage in an extra high voltage substation connector. *IEEE Trans. Dielectr. Electr. Insul.* **2013**, *20*, 82–88. [CrossRef]
11. Ilhan, S.; Ozdemir, A. 380 kV Corona Ring Optimization for ac Voltages. *IEEE Trans. Dielectr. Electr. Insul.* **2011**, *18*, 408–417. [CrossRef]
12. Diaz-Acevedo, J.A.; Escobar, A.; Grisales-Norena, L.F. Optimization of corona ring for 230 kV polymeric insulator based on finite element method and PSO algorithm. *Electr. Power Syst. Res.* **2021**, *201*, 107521. [CrossRef]
13. Alti, N.; Bayadi, A.; Belhouchet, K. Grading ring parameters optimization for 220 kV metal-oxide arrester using 3D-FEM method and bat algorithm. *IET Sci. Meas. Technol.* **2021**, *15*, 14–24. [CrossRef]
14. M'hamdi, B.; Teguar, M.; Mekhaldi, A. Optimal design of corona ring on HV composite insulator using PSO approach with dynamic population size. *IEEE Trans. Dielectr. Electr. Insul.* **2016**, *23*, 1048–1057. [CrossRef]
15. Zhang, S.; Peng, Z.; Peng, L.; Wang, H. Optimization of Corona Ring Structure for UHV Composite Insulator Using Finite Element Method and PSO Algorithm. In Proceedings of the 2013 IEEE International Conference on Solid Dielectrics (ICSD 2013), Bologna, Italy, 30 June–4 July 2013; pp. 210–213. [CrossRef]
16. Terrab, H.; Kara, A. Parameters design optimization of 230 kV corona ring based on electric field analysis and response surface methodology. *Electr. Power Syst. Res.* **2018**, *163*, 782–788. [CrossRef]
17. Zachariades, C.; Rowland, S.M.; Cotton, I.; Peesapati, V.; Chambers, D. Development of Electric-Field Stress Control Devices for a 132 kV Insulating Cross-Arm Using Finite-Element Analysis. *IEEE Trans. Power Deliv.* **2016**, *31*, 2105–2113. [CrossRef]
18. Sardast, R.; Faghihi, F.; Vakilian, M. Study on Different Dimensions of C-type Corona Rings in 400 kV Insulator Strings Based on FEM Analysis of Electric Field Distribution. In Proceedings of the 2019 27th Iranian Conference on Electrical Engineering (ICEE 2019), Yazd, Iran, 30 April–2 May 2019; pp. 673–678. [CrossRef]
19. Hernandez-Guiteras, J.; Riba, J.; Romeral, L. Redesign process of a 765 kV (RMS) AC substation connector by means of 3D-FEM simulations. *Simul. Model. Pract. Theory* **2014**, *42*, 1–11. [CrossRef]
20. Pattanadech, N.; Potivejkul, S.; Yuttagowit, P. Corona phenomena of various high voltage shielding types. In Proceedings of the 2006 International Conference on Power System Technology, Chongqing, China, 22–26 October 2006; pp. 1–6. [CrossRef]
21. Liao, J.; Peng, Z.; Li, N.; Wu, H. E-Field distribution of circuit with value controlled reactors in 750 kV substations. In Proceedings of the 2015 IEEE 11th International Conference on the Properties and Applications of Dielectric Materials (ICPADM), Sydney, NSW, Australia, 19–22 July 2015; pp. 572–575. [CrossRef]

22. Liu, Z.; Li, W.-D.; Wang, Y.-B.; Su, G.-Q.; Zhang, G.-J.; Cao, Y.; Li, D.-C. Topology optimization and 3D-printing fabrication feasibility of high voltage FGM insulator. In Proceedings of the 2016 IEEE International Conference on High Voltage Engineering and Application (ICHVE), Chengdu, China, 19–22 September 2016; pp. 1–4. [CrossRef]
23. Wei-Chung, L.; Caldwell, D.W. Apparatus for Preventing Coronal Discharge. 2000. US09. 8. Available online: https://www.uspto.gov (accessed on 31 July 2022).
24. Deaconu, S.; Coleman, H.W. Limitations of Statistical Design of Experiments Approaches in Engineering Testing. *J. Fluids Eng.* **2000**, *122*, 254–259. [CrossRef]
25. Riba, J.; Abomailek, C.; Casals-Torrens, P.; Capelli, F. Simplification and cost reduction of visual corona tests. *IET Gener. Transm. Distrib.* **2018**, *12*, 834–841. [CrossRef]
26. *International Electrotechnical Commission IEC 61284: 1997 Overhead Lines-Requirements and Tests for Fittings*; International Electrotechnical Commission: Geneva, Switzerland, 1997; p. 17.